Supporting Information

Giant Electric Field Enhancement and Localized Surface Plasmon Resonance by Optimizing Contour Bowtie Nanoantenna

Li-Wei Nien,[†] *Shih-Che Lin,*[†] *Bo-Kai Chao,*[†] *Miin-Jang Chen,*[†] *Jia-Han Li,*[‡] *and Chun-Hway Hsueh*[†,]*

[†]Department of Materials Science and Engineering and [‡]Department of Engineering Science and Ocean Engineering, National Taiwan University, Taipei 10617, Taiwan

*Corresponding Author: hsuehc@ntu.edu.tw

Charge Distributions on Contour Bowtie Antenna

The charge distributions on the contour bowtie antenna NCB100 with the *t/R* ratio of 0.3 (i.e., t = 30 nm) at the resonance wavelengths of λ = 1156, 911, 690 and 530 nm can also be obtained from FDTD simulations and are shown in Figure S1. The results shown in Figure S1 are in good qualitative agreement with those in Figure 6 which were derived from the electromagnetic fields and phase profiles shown in Figure 5 and Eq. (4). However, a minor difference in the charge distributions is noted at the end of the cavity bowtie between Figure 6(c) and Figure S1(c) for λ = 911 nm. While both show that the charge distributions are close to zero at the end of the cavity bowtie, Figure 6(c) exhibits slightly positive but Figure S1(c) exhibits

slightly negative. This discrepancy could result from the fact that only the electric field in the polarization direction, E_x, was considered in deriving the results in Figure 6(c) and the three components of the electric field were considered in using the numerical simulation to derive the results in Figure S1(c). Because the E_x intensity at the end of the cavity bowtie is very small compared to that at the opposing apex (see Figure 5(c)), neglect of E_y and E_z could result in inaccuract results. Nevertheless, it is sufficient to consider only E_x in deriving the charge distribution for most of the cases as revealed by the good qualitative agreement between Figure 6 and Figure S1.

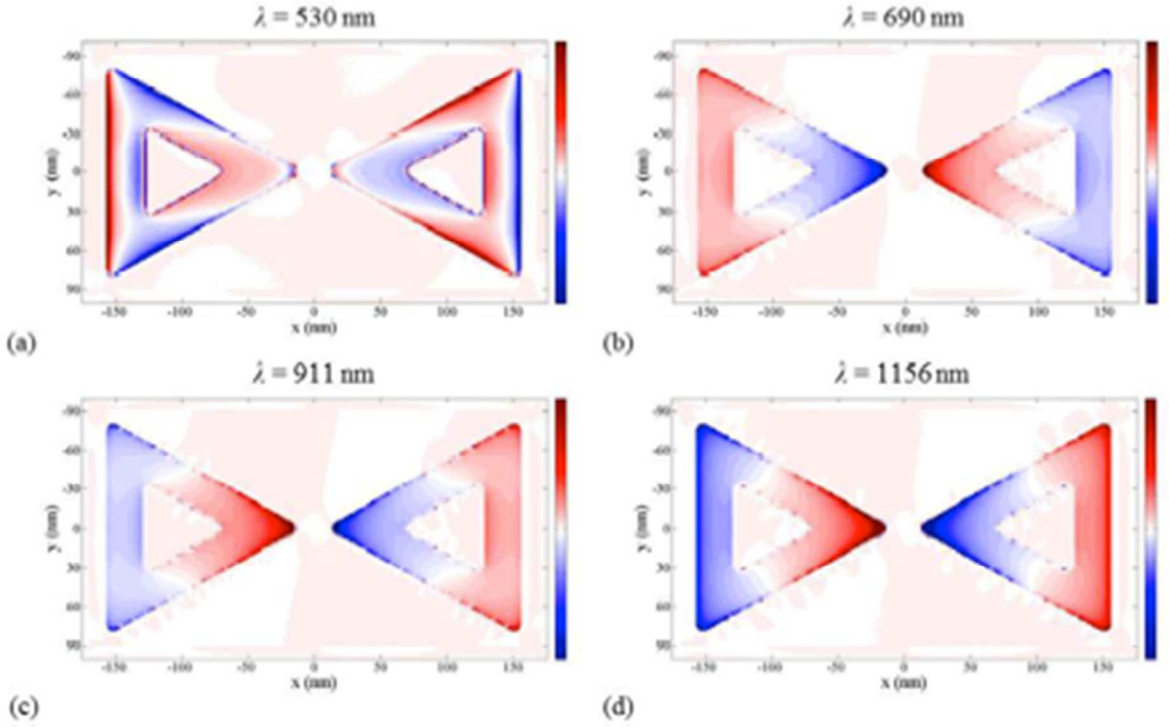

Figure S1. FDTD simulated charge distributions on the contour bowtie antenna NCB100 with the *t/R* ratio of 0.3 at the resonance wavelengths of (a) λ = 530 nm, (b) λ = 690 nm, (c) λ = 911

nm, and (d) λ = 1156 nm. The red and the blue colors represent the positive and the negative charges, respectively.

Verification of the proposed plasmon hybridization model for the contour bowtie antenna can also be achieved by examining charge distributions as shown in Figure S2 for the case of NCB100 with the *t/R* ratio of 0.3. For solid NCB100, there are two plasmon resonances as dipole and quadrupole resonances, respectively, at the longer (921 nm) and the shorter wavelengths (617 nm), and the corresponding charge distributions are shown in the left column of Figure S2. For the plasmon resonances of the contour bowtie antenna at λ = 1156 and 911 nm, they can be deduced from the hybridization of the resonance of solid bowtie antenna at λ = 921 nm with the cavity bowtie structure at λ = 886 nm. In the contour bowtie region, the charge distributions of the contour bowtie antenna at λ = 1156 and 911 nm are similar to that of the solid NCB100 at λ = 921 nm. In this case, the plasmonic behavior of the contour bowtie antenna is dominated by the charges induced by the solid bowtie structure and slightly influenced by the cavity plasmon resonance. In the same way, for the plasmon resonances of the contour bowtie antenna at λ = 690 and 530 nm, they are hybridized from the resonance modes of the solid bowtie antenna at λ = 617 nm and the cavity bowtie structure at λ = 620 nm.

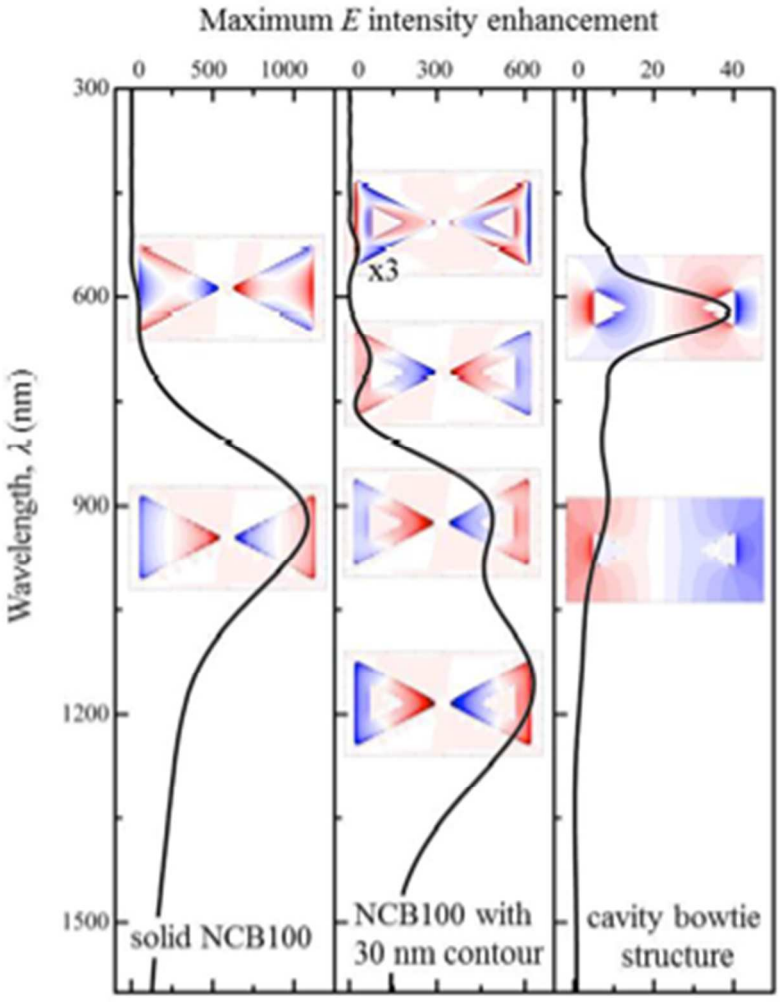

Figure S2. Maximum *E* intensity enhancement for NCB100 with 30 nm contour thickness (*t*/*R* ratio of 0.3) (middle), which is hybridized from the interaction between solid NCB100 (left) and cavity bowtie structure (right) and the corresponding charge distributions for each resonance mode.